HHS Public Access

Author manuscript

J Comp Neurol. Author manuscript; available in PMC 2022 April 28.

Published in final edited form as:

J Comp Neurol. 1993 October 15; 336(3): 321–330. doi:10.1002/cne.903360302.

Glutamatergic and Cholinergic Projections to the Pontine Inhibitory Area Identified With Horseradish Peroxidase Retrograde Transport and Immunohistochemistry

Y.Y. LAI,

Department of Psychiatry and Brain Research Institute, School of Medicine, UCLA, Los Angeles, California 90024, Neurobiology Research, VA Medical Center, Sepulveda, California 91343

J.R. CLEMENTS,

Department of Veterinary Anatomy, Texas A&M University, College Station, Texas 77843

J.M. SIEGEL

Department of Psychiatry and Brain Research Institute, School of Medicine, UCLA, Los Angeles, California 90024, Neurobiology Research, VA Medical Center, Sepulveda, California 91343

Abstract

Previous studies in our laboratory have shown that microinjection of acetylcholine and non-N-methyl-D-aspartate (NMDA) glutamate agonists into the pontine inhibitory area (PIA) induce muscle atonia. The present experiment was designed to identify the PIA afferents that could be responsible for these effects, by use of retrograde transport of wheat germ agglutinin conjugated horseradish peroxidase (WGA-HRP), glutamate immunohistochemistry and NADPH-diaphorase staining techniques. Experiments were performed in both decerebrate and intact cats. Dense retrograde WGA-HRP labelling was found in neurons in the periaqueductal gray (PAG) and mesencephalic reticular formation (MRF) at the red nucleus (RN) level, ventral portion of paralemniscal tegmental field (vFTP), retrorubral nucleus (RRN), contralateral side of PIA (cPIA), pontis reticularis centralis caudalis (PoC), and most rostral portion of the nucleus parvicellularis (NPV) and nucleus praepositus hypoglossi (PH) at the level of the pontomedullary junction; moderate labelling was seen in pedunculopontine nucleus, pars compacta (PPNc), laterodorsal tegmental nucleus (LDT), superior colliculus (SC), MRF and PAG at the level caudal to RN, medial and superior vestibular nuclei, and principle sensory trigeminal nucleus (5P); and light labelling was seen in dorsal raphe (DR) and locus coeruleus complex (LCC). The projection neurons were predominantly ipsilateral to the injection site, except for both vFTP and RRN, which had more projection cells on the contralateral side. Double labelled WGA-HRP/NADPH-d neurons could be found in PPNc and LDT. Double labelled WGA-HRP/glutamatergic neurons could be seen at high densities in MRF, RRN, vFTP, and cPIA, moderate densities in SC, LDT, PPNc, PoC, and NPV, and low densities in PH, 5P, DR, LCC, and PAG. No cells in LDT and PPNc were triple labelled with NADPH-d, glutamate antibody and WGA-HRP. The mesopontine efferents identified here may mediate the suppression of muscle tone in REM sleep and coordinate muscle tone during head and neck movements.

Address reprint requests to Y.Y. Lai, Neurobiology Research (151A3), VA Medical Center, Sepulveda, CA 91343.

Keywords

glutamate; acetylcholine; atonia; REM sleep; pons

Microinjection of cholinergic agonists into the pontine inhibitory area (PIA), which includes nucleus reticularis pontis oralis (PoO) and rostral portion of the nucleus reticularis pontis caudalis (PoC), produces muscle atonia and REM sleep-like activity (George et al., ’64; van Dongen et al., ’78; Shiromani et al., ’86; Vanni-Mercier et al., ’89). Recently, we found that not only acetylcholine but also glutamate agonists injected in this area suppress muscle tone in decerebrate cats (Lai and Siegel, ’88). This muscle tone suppression was found to be mediated by non-N-methyl-D-aspartate (NMDA) receptors (Lai and Siegel, ’88). Furthermore, NMDA and non-NMDA agonist injections into the same or nearby sites in PIA produced opposite effects on muscle activity, with increases in tone and/or locomotion induced by NMDA agonists and decreases in tone induced by non-NMDA agonists (Lai and Siegel, ’91).

Descending pathways originating from the PIA were found in the nucleus magnocellularis (NMC) of the medulla and spinal cord (Tohyama et al., ’79; Sakai, ’80). However, the afferents to the PIA are poorly understood. Electrophysiological studies by McCarley et al. (’87) found that 75–86% of the neurons in PIA responded monosynaptically to stimulation of the contralateral PIA and mesencephalic reticular formation (MRF). Anatomical studies demonstrated that cholinergic neurons in the lateral dorsal tegmental (LDT) and pedunculopontine (PPN) nuclei project to PIA (Mitani et al., ’88; Shiromani et al., ’88; Quattrochi et al., ’89; Semba et al., ’90). However, the sources of glutamatergic afferents that can induce muscle atonia in PIA are unknown. The combining of wheat germ agglutinin conjugated horseradish peroxidase (WGA-HRP), immunocytochemical, and nicotinamide adenine dinucleotide phosphate diaphorase (NADPH-d) staining techniques in this experiment was designed to determine the rostral brainstem glutamatergic afferents to PIA and their relation to the cholinergic afferents to this region.

MATERIALS AND METHODS

Eight cats of either sex weighing 3–4 kg were used. Three were decerebrated and physiological recording was performed before WGA-HRP injection. Five cats were intact, and WGA-HRP injection was made without prior recording.

Preparation of decerebrate cats

Decerebration was done as described previously (Lai and Siegel, ’89). Under halothane anesthesia the carotid arteries were ligated, and brain structures rostral to the superior colliculus were removed. The bony tentorium was removed to allow injections into the PIA in the coronal stereotaxic plane. Individual neck muscles were dissected and implanted with bipolar electrodes for electromyograph (EMG) recording. Train stimulation of 500 ms (100 Hz, 0.2 ms, and 20–50 μA cathodal pulses) was applied through a stainless monopolar microelectrode (A-M Systems, model 5710) to the pontine reticular formation to identify the inhibitory area (Lai and Siegel, ’88). After removal of the recording electrode, 0.5 μl

of either quisqualate (10 mM) or acetylcholine (1 M) was microinjected through a 25 Gs Hamilton 1 μ1 microsyringe (7001) to confirm the neurotransmitter specificity of the effect. WGA-HRP was injected into the PIA 1 hour after prior injections. Only sites at which muscle suppression was produced by chemical injection were used for WGA-HRP injection. Supplemental lactated Ringer's saline solution was given subcutaneously twice a day.

Preparation of intact cats

Cats were anesthetized with Nembutal (30 mg/kg, intraperitoneally). A small hole was made in the skull over the cerebellum for WGA-HRP injection. The injection cannula was guided down to the PIA with a manipulator angled at 45° from the coronal plane.

WGA-HRP injection and perfusion

Fifty nanoliters of 2.5% WGA-HRP were injected through a 1 μl Hamilton microsyringe over 5 minutes. In all cases, a single unilateral injection was made. Cats were killed 48 hours after injection by perfusion, following the protocol for WGA-HRP and immunocytochemical studies with 1 liter of Ringer's saline, followed by 2 liters of 3% paraformaldehyde and 0.25% glutaraldehyde in 0.1 M phosphate buffer solution, pH 7.4. All solutions were at 10°C. The brainstems were removed and postfixed in 3% paraformaldehyde in 0.1 M phosphate buffer, pH 7.4, for 2 hours at 4°C. Then, brain tissues were transferred through increasing concentrations of sucrose solution prior to sectioning on either a freezing or vibrating microtome.

WGA-HRP staining and immunocytochemical technique

The brain tissues were cut coronally at 50 μm. Sequential sections were processed as described below for NADPH-d; WGA-HRP; glutamate immunoreactivity; NADPH-d and WGA-HRP; WGA-HRP and glutamate immunoreactivity; and NADPH-d, glutamate, and WGA-HRP.

Neurons containing nitric oxide synthase (Vincent and Kimura, '92) were histochemically identified with an NADPH-d technique that is a modification of the method of Scherer-Singler (Scherer-Singler et al., '83). Sections were collected into 0.1 M phosphate buffer (pH 7.4, 4°C) and incubated immediately after cutting in a solution containing 15 mM sodium malate, 1 mM NADPH, 20 mM $MgCl_2$, and 0.2 M nitro blue tetrazolium in 0.1 M Tris-HC1 (pH 8.0) for 15–30 minutes at 37°C in the dark. Sections were rinsed in 0.1 M Tris buffer and mounted.

Retrogradely transported WGA-HRP was visualized with tetramethyl benzidine (TMB) as the final reaction product (Mesulam, '78). Then, the TMB product was stabilized by incubation in a combination of diaminobenzidine (DAB), cobalt chloride, and hydrogen peroxide (Rye et al., '84). Five minutes after incubation, sections were rinsed with cold phosphate buffered saline (PBS).

For glutamate immunohistochemistry, sections were rinsed in 0.1 M PBS (pH 7.4), incubated for 30 minutes in normal goat serum, and then incubated for 18 hours at 4°C in a 1:15,000 dilution of a polyclonal antibody raised against glutamate conjugated to a

carrier protein hemocyanin with glutaraldehyde (Hepler et al., ’88) obtained from Arne1 Products. Following incubation in the primary antibody, the sections were rinsed in PBS and incubated sequentially in biotinylated goat anti-rabbit antisera, acetyl-avidinbiotinylated peroxidase complex (Vector Laboratories, Inc., Burlingame, CAI, and 0.05% DAB with 0.02% hydrogen peroxide. Tissue sections were rinsed in PBS between incubations, and all incubations, except for that of the primary antibody, were performed at 20°C.

The combination of these three protocols resulted in the deposition of a black, crystalline reaction product in projection neurons, a brown, homogeneous reaction product over glutamate-like immunoreactive neurons and a homogeneous blue reaction product in NADPH-d neurons (see Fig. 4). Thus, single, double, and triple labelled neurons could be distinguished and identified.

RESULTS

In all the experiments described here in decerebrate and intact animals, the center of the injection site was located in PIA, from P 1.5 to 3, L 2–3. However, the dorsal trajectory differed in these two preparations, with trace amounts of WGA-HRP deposited along a straight dorsoventral extension in the decerebrate and a dorsocaudal to ventrorostral extension in the intact animals. Two examples of the location of the injection site are illustrated in Figure 1. Both acetylcholine or non-NMDA agonist injections in this area in the decerebrate cat produced bilateral suppression of neck muscle tone as previously reported (Lai and Siegel, ’88).

General observations

There was no difference between the distribution of labelled cells in caudal midbrain and pons in decerebrate and intact animals. However, since the rostra1 midbrain was not well perfused due to ligation of the carotid arteries, histochemical and immunocytochemical labelling was reduced in this area in the decerebrate cat. Therefore, the descriptions of midbrain labelling are based primarily on observations from intact animals injected with WGA-HRP.

Most of the retrograde WGA-HRP labelled cells were small to medium, with few large ones. No giant cell was labelled with WGA-HRP. A small neuron was defined as one whose soma major axis ranges from 10 to 25 μm. The soma smajor axis for medium and large neurons was 26–35 and 36–45 μm, respectively. A giant neuron was one with soma major axis exceeding 46 μm.

Neurons retrogradely labelled with WGA-HRP were located throughout the mesopontine reticular formation (Figs. 2, 3; Table 1). In the midbrain at the level of the red nucleus (RN), concentrations of labelled WGA-HRP neurons were found in the ipsilateral side of periaqueductal gray (PAG) and mesencephalic reticular formation (MRF); moderate labelling in contralateral MRF and ipsilateral superior colliculus (SC); and light labelling in contralateral side of SC and PAG. Caudal to RN, very heavy retrograde WGA-HRP labelling was found in both sides of the retrorubra1 nucleus (RRN); heavy labelling in the ipsilateral MRF; and light labelling in dorsal raphe nucleus (DR) and contralateral MRF. At

the mesopontine junction and pons, dense concentrations of WGA-HRP positive cells could be found in both sides of the ventral part of the paralemniscal tegmental field (vFTP), the contralateral side of the pontine inhibitory area (cPIA) and PoC, and the ipsilateral side of nucleus parvicellularis (NPV) and nucleus praepositus hypoglossi (PH); moderate labelling was seen in the ipsilateral side of LDT and PPN, superior and medial vestibular nuclei (SVN and MVN), and principle sensory trigeminal nucleus (5P); and light labelling in the contralateral side of PAG, LDT, PPN, locus coeruleus complex (LCC), and DR.

Since cholinergic neurons in LDT and PPN synthesize nitric oxide, the NADPH-d stain effectively labels cholinergic neurons in this area. Cells in other regions of brainstem, such as PAG, MRF, and PIA also contain nitric oxide synthase, but do not contain choline acetylsynthase (Vincent and Kimura, ’92). To identify cholinergic neurons, we therefore plotted only those NADPH-d neurons in the LDT-PPN region. Double labelled cells positive for both NADPH-d and WGA-HRP were found in both LDT and PPN (Figs. 2, 3) although the number was small (Table 1). Neurons containing both glutamate and WGA-HRP staining were located throughout the brainstem extending from the midbrain to the pontine reticular formation. A large number of double labelled neurons were observed in MRF, RRN, vFTP, cPIA, and PoC. A relatively small number of glutamatergic/WGA-HRP cells was found in LDT, PPN, and PAG. A very small number of WGA-HRP/glutamatergic neurons was located in NPV, 5P, SVN, MVN, and SC.

Retrorubral nucleus (RRN)

WGA-HRP neurons were seen in both sides of RRN, with more projection cells from contralateral than ipsilateral side. A large concentration of small to medium size, multipolar or spindle-shaped with elongated neuronal process projection cells (Fig. 4c) were located in this area. Forty-six percent of the projection cells were glutamatergic.

Mesencephalic reticular formation (MRF; FTC)

Retrogradely labelled cells could be found in both sides of MRF, but the majority of projection cells were located ipsilaterally. At the level of trochlear nucleus, more projection neurons were found after rostral injection than after caudal injection (Fig. 2). However, in both rostral and caudal injections, concentrations of WGA-HRP neurons were found in the area ventral to PAG and SC at the level of substantia nigra, and ran through the entire MRF at more caudal levels. At the mesopontine junction level, the distribution of projection cells was different after rostral and caudal WGA-HRP injections (Fig. 2). A high concentration of WGA-HRP neurons could be seen after rostral injections; however, only a small number of projection neurons was seen after caudal injections. Single WGA-HRP labelled cells were small, medium, and large in size. The medium and large projection cells had multipolar processes; however, the small cells were spindle-shaped. Forty-seven percent of these projection neurons were also glutamatergic.

Superior colliculus (SC)

The projection cells in SC were predominantly ipsilateral to the injection site. On the ipsilateral side, retrogradely labelled cells were located mostly in the intermediate and the deep layers of the nucleus (Berman, ’68). Projection neurons extended from dorsolateral

to medioventral in a discrete band. Contralaterally, projection neurons were found in the rostral portion of the deep layer, with a few in the intermediate layer of the nucleus. Most of the projection neurons were small and spindle shaped. A few large multipolar projection neurons were located in the intermediate layer of the SC. Twenty-three percent of retrograde WGA-HRP cells were also stained with glutamate.

Periaqueductal gray (PAG)

Almost all of the projection cells were ipsilateral to the injection site. Ipsilaterally, retrograde cells were clustered in two distinct areas. In the dorsomedial PAG near the midline, a high density of WGA-HRP cells was found in the midbrain, with a few at the pontine level. The neurons in this area were small and oval or spindle-shaped. Another projection area included the dorsolateral and the entire ventral region of the PAG. The WGA-HRP stained neurons in this portion of PAG were more numerous at the midbrain level than at the pontine level. The projection neurons were small to large in size. Neurons located in the lateral portion were medium to large in size, with several neuronal processes. However, neurons in the medial portion were small, with a round or spindle shape. As in the MRF, the number of the projection neurons in PAG at the mesopontine junction was greater after our rostral injection than after our caudal injections. Contralaterally, the number of retrogradely labelled neurons was small, and they were scattered in the lateral and ventral portions at the red nucleus level and in the ventrolateral portion of the nucleus at the pontine level. Retrogradely labelled neurons were small to medium size and spindle shaped. Double labelled WGA-HRP/glutamatergic neurons made up 32% of projection neurons, and most of them were located in ventral portion of the PAG.

Dorsal raphe nucleus (DR)

A small number of projection cells were found in DR and they were predominantly located ipsilateral to the injection site (Figs. 2, 3). Most of the WGA-HRP cells were medium size with multipolar precesses. Approximately 36% of projection cells were also glutamate labelled.

Lateral dorsal tegmentum (LDT)

The majority of projection cells were found ipsilateral to the injection site (Figs. 2, 3). Small, medium, and large size cells were labelled in this nucleus. The size of the neurons was found to correlate with the transmitter and projection pattern. Most of the single labelled WGA-HRP cells were small and fusiform. Double labelled glutamatergic/WGA-HRP cells were small to medium sized, with round, fusiform, or oligopolar processes. Double labelled WGA-HRP/NADPH-d cells were large in size (Fig. 4e). Overall, the size of single labelled WGA-HRP projection cells in LDT was smaller than that of NADPH-d cells. Although some neurons labelled for both NADPH-d and glutamate, these double labelled cells did not project to the PIA. Thirteen percent of ipsilateral and 22% of contralateral cells projecting to PIA had NADPH-d positive staining. However, the percentage of double labelled WGA-HRP/glutamatergic neurons was higher than the WGA-HRP/NADPH-d neurons. Among the cells projecting to PIA, 35% of ipsilateral and 17% of contralateral cells were found to be glutamatergic.

Pedunculopontine nucleus, pars compacta (PPNc)

Consistent with the observations of Moon Edley and Graybiel (’83), we saw no distinct cytoarchitectural boundaries in the cat’s PPN. Therefore, the area of PPNc described in this experiment included the cholinergic neurons area ventral and lateral to the nucleus cuneiformis. As in the LDT, projection cells were more numerous on the ipsilateral side. As seen in the LDT, single labelled WGA-HRP cells were small to medium sized (Fig. 4a,b) and had one to three dendritic processes. Double labelled NADPH-d/WGA-HRP cells could be found from rostral to caudal PPNc (Figs. 2, 3), although the number was small. The percentage of the projection cells that also contained NADPH-d staining was 22% in contralateral and 13% in ipsilateral PPNc. Most of the NADPH-d/WGA-HRP cells contained multipolar processes and were medium sized. Small to medium sized neurons containing both glutamatergic and WGA-HRP staining were found throughout the nucleus (Figs. 2, 3). The smaller cells had monopolar or oligopolar processes, while spindle shaped dipolar and multipolar neurons were larger in diameter. The double labelled WGA-HRP/glutamatergic neurons made up 26% of the contralateral and 53% of the ipsilateral projection neurons. As in the LDT, some neurons were double labelled with NADPH-d and glutamate (Fig. 4h,i); however, no neuron stained with WGA-HRP, NADPH-d, and glutamate.

Paralemniscal tegmental field (FTP)

Large numbers of WGA-HRP labelled cells could be observed in this area, and most of them were located in the ventral portion of the FTP (Fig. 2). Like the RRN, the majority of projection cells were located contralateral to the injection. Single labelled WGA-HRP cells were small to large size, with multipolar processes, and could be seen in the ventrolateral area. Single labelled glutamatergic cells were small in size. However, double labelled glutamatergic/WGA-HRP cells were small to large in size, with a spindle shape or with multipolar processes. This double labelled cell type was found mostly in the ventral part of FTP (vFTP). The vFTP could be divided into several subregions according to the distribution and size of projection cells (Fig. 4l). The most ventral area was compact and had small to medium size neurons. In the lateral part of the vFTP, the nucleus was compact, with small to large neurons intermixed. The distribution of the projection cells in the medioventral part of the vFTP was very diffuse. Small to large neurons could be seen in this area. Fifty percent of the projection cells in the entire area of FTP were also stained with glutamate (Table 1). Pale blue NADPH-d positive cells could be also seen in FTP with single or double labelling with either WGA-HRP or glutamate. The single labelled NADPH-d positive cells were small with oval shape and double labelled cells were medium to large in size with multipolar processes.

Contralateral side of pontine inhibitory area (cPIA)

Dense retrograde WGA-HRP and double labelled glutamate cells were present in this area (Fig. 3). More than 90% of the retrogradely labelled cells contained glutamate. The area containing WGA-HRP cells was symmetrical with the injection site. Very heavily labelled WGA-HRP stained crossing fibers could be seen in the midline of the pons (Fig. 4k). The

projection cells were small to large in size. Most of them had several elongated neuronal processes. No giant neuron was found to be WGA-HRP stained (Fig. 4d).

Locus coeruleus complex (LCC)

A few projection neurons were seen in LCC (Fig. 3). Most of the projection cells were found in the medioventral portion of the LCC corresponding to the nucleus subcoeruleus. The projection cells were of medium size and spindleshaped or contained multipolar neuronal processes. Some of the WGA-HRP cells were also stained with glutamate.

Nucleus reticularis pontis caudalis (PoC)

A very intense projection was found from the contralatera1 side of the PoC. However, the distribution of the projection cells on the ipsilateral side at the rostral superior olive nucleus level depended on the injection site. The caudal site injection produced moderate while the rostral site injection had a light retrograde labelling (Fig. 3). The size of the projection neurons was small to large (Fig. 4g), with most of the large projection neurons located in the ventral portion of the nucleus. No giant neuron was stained with TMB. The small neurons were spindle shaped, and medium and large neurons had several neuronal processes. Double labelled WGA-HRP and NADPH-d positive neurons were found, although the neurochemical role of NADPH-d cells in this area is unclear. Some of the WGA-HRP cells were also double labelled with glutamate. The double labelled glutamate neurons made up 30% of the projection.

Principle sensory trigeminal nucleus (5P)

A moderate density of WGA-HRP labelled neurons was found in 5P. In the contralateral side, the projection neurons were exclusively from the ventral division of the 5P, while in the ipsilateral side, WGA-HRP neurons could be seen in both of the dorsal and ventral divisions. The projection neurons were small to large in size with a few neuronal processes. Double labelled glutamate and WGA-HRP neurons made up 30% of the projections.

Pontomedullary junction

Since the medullary reticular formation of the brainstem was not available, the data of the following neuronal structures were exclusively from the most rostral portion of these nuclei at the level of the pontomedullary junction.

Nucleus parvicellularis (NPV)

The projection neurons were found predominantly on the ipsilateral side. The ipsilateral side of the NPV had a very heavy projection to the PIA. Most of the WGA-HRP cells had a small size and were round or spindle shaped. Some of the projection neurons were medium size with few neuronal processes. Double labelled glutamate/WGA-HRP neurons made up 18% of the projection cells.

Medial and superior vestibular nuclei (MVN, SVN)

A moderate density of projection neurons was found in both sides of MVN and SVN. In the MVN, most of the WGA-HRP cells were found in the ventrolateral portion of the

nucleus, near the junction of the MVN and SVN. However, WGA-HRP neurons were found throughout the SVN. The size of the projection neurons in MVN was small, whereas most of the neurons were medium to large in SVN. No glutamatergic neurons in MVN were found to project to the PIA. However, double labelled glutamate and WGA-HRP neurons made up 20% of the projections in the SVN.

Nucleus praepositus hypoglossi (PH)

The projection from the PH was found to be exclusively from the contralateral side (Fig. 3). WGA-HRP neurons were small in size and had a round shape or a few short dendritic processes. No glutamatergic neuron stained with TMB.

DISCUSSION

In accord with the results of physiological studies, the afferent projections from rostral areas of brainstem to PIA included many regions that have been found to be related to motor and REM sleep expression systems. The mesopontine reticular formation that we previously found to suppress muscle tone when electrically stimulated (Lai and Siegel, ’90) had moderate to heavy projections to PIA. Our physiological studies demonstrated that both glutamate and cholinergic agonists microinjected into PIA induced muscle atonia (Lai and Siegel, ’88), a characteristic of REM sleep. The current anatomical studies indicated that glutamatergic and cholinergic inputs to this area originate in separate projection neurons in mesopontine reticular formation.

Specificity of glutamate-like immunoreactivity

Four different pools of glutamate, the transmitter pool, the glial pool, the gamma-aminobutyric acid (GABA) precursor pool, and the metabolic pool, have been defined (Fonnum, ’91). The highly specific antiserum raised against glutamate that has recently been developed (Beitz et al., ’86; Hepler et al., ’86) allows the visualization of putative glutamatergic neurons in the CNS. It is to be expected that all structures containing glutamate will have some staining with this antibody. However, the levels of immunolabelling in certain cells were greatly enhanced relative to other cells. Such a pattern of labelling is what one would expect for the transmitter pool, although further work is needed to prove that the labelled cells use glutamate as a transmitter. Our physiological studies have shown that the PIA is responsive to glutamate, with microinjection of non-NMDA agonists inducing muscle atonia (Lai and Siegel, ’91). The sources of glutamatergic projections to the PIA that we identified in the present study also triggered muscle suppression by electrical stimulation (Lai and Siegel, ’90). Thus, we hypothesize that the glutamate immunolabelled projections to PIA identified here are the endogenous source for activation of the glutamate receptors we identified in PIA.

Origin of brainstem projections to the PIA

Most of the projection cells in the present study were glutamatergic neurons. The major inhibitory areas in the pontomesencephalic reticular formation that we identified with electrical stimulation (Lai and Siegel, ’90) had moderate to dense projections to PIA. These areas include RRN, MRF, vFTP, and PPNc. All of these areas had a high percentage

of double labelled glutamatergic/WGA-HRP cells. Cholinergic projection neurons were found in PPNc and LDT areas only. Since no triple labelled glutamatergic, ACh, and WGA-HRP cells in LDT or PPNc were found, we suggest that the majority of glutamatergic and cholinergic inputs that participate in the induction of muscle atonia in PIA come from segregated populations of neurons containing either glutamate or acetylcholine. The distribution of the projection from midbrain and pons to PIA in cat in the present study is similar to the previous reports of Shammah-Lagnado et al. (’87) in the rat and Semba et al. (’90) in the cat. However, Shammah-Lagnado et al. reported that only a few cells in LDT and PPNc projected to PIA. The sources of cholinergic inputs to PIA that we found in the present studies were in LDT and PPNc, in accord with the studies of the others (Mitani et al., ’88; Shiromani et al., ’88; Quattrochi et al., ’89; Semba et al., ’90). However, in contrast to Shiromani et al.’s finding that only 5% of the projection neurons from LDT and PPNc to PIA were not choline acetyltransferase immunoreactive, we found that the majority of projection neurons from LDT and PPNc to PIA did not stain for NADPH-d. The discrepancy between these two studies might be due to differences in staining techniques used for cholinergic cells. Although Vincent et al. (’86) found that the NADPH-d staining of cholinergic neurons in LDT and PPNc in the rat matched the choline acetyltransferase (ChAT) immunocytochemical staining, approximately 10% of NADPH-d positive cells in the human were ChAT negative (Mesulam et al., ’89). However, the distribution of the NADPH-d positive and ChAT immunoreactive neurons was identical in both LDT and PPN areas in the cat (Reiner and Vincent, ’87). One possible explanation for the difference in our findings and those of Shiromani et al. is a greater sensitivity of our retrograde staining procedure.

Pale blue NADPH-d positive neurons were found in several different areas of the brainstem. These areas included PAG, MRF, SC, vFTP, RRN, PoC, and PIA. Some of the NADPH-d positive cells in those areas were also double stained with WGA-HRP. The NADPH-d histochemical technique had been found to stain neurons that contained nitric oxide synthase (Vincent and Kimura, ’92).

In contrast to the cholinergic inputs to the PIA, which came from LDT and PPNc, the glutamatergic projection neurons were widespread in the brainstem. The number and percentage of double labelled WGA-HRP glutamatergic cells were greater than that of double labelled NADPH-d cells.

Functional implications

We had reported that cholinergic and glutamatergic agonists microinjected into PIA induced muscle atonia in decerebrate cat (Lai and Siegel, ’88). Furthermore, we found that NMDA and non-NMDA glutamate agonist injections into the same region of PIA produced opposite effects on muscle tone, with muscle atonia produced by non-NMDA and muscle facilitation and/or locomotion by NMDA injections (Lai and Siegel, ’91). Our previous electrophysiological studies also demonstrated that electrical stimulation in RRN, vFTP, and PPNc produced muscle suppression (Lai and Siegel, ’90). Repetitive stimulation in some areas, such as PPNc and vFTP, not only produced muscle suppression during stimulation but also induced locomotion after stimulations. The present studies, which

showed the distribution of double labelled glutamate and WGA-HRP neurons projecting to PIA, provides the anatomical substrate for our physiological findings.

REM behavioral disorder was described as motor hyperactivity superimposed with or without muscle atonia during REM sleep (Schenck et al., ’92). Although the majority of REM behavioral disorder cases were idiopathic, some cases were associated with mesopontine lesions (Schenck and Mahowald, ’90). Our present anatomical and previous physiological results (Lai and Siegel, ’91) reveal a circuit that could underlie the muscle tone suppression of REM sleep and its disturbance in the REM behavioral disorder. Hyperactivity of this circuit produces cataplexy, which is caused by the triggering of the atonia circuit in waking (Siegel et al., ’91, ’92). In both narcolepsy and idiopathic REM behavior disorder, the locus of the pathology within this circuit remains to be determined.

ACKNOWLEDGMENTS

This work was supported by the Medical Research Service of the Veterans Administration and by PHS grants HL41370 and NS14610.

Abbreviations

AQ	aqueduct
BC	brachiurn conjunctivum
CNF	nucleus cuneiformis
CPIA	contralateral pontine inhibitory area
Cs	superior central nucleus
DR	dorsal raphe
FTC	central tegmental field
FTP	paralemniscal tegmental field
IC	inferior colliculus
IP	interpeduncular nucleus
LC	nucleus locus coeruleus
LDT	lateral dorsal tegmentum
MRF	mesencephalic reticular formation
MVN	medial vestibular nucleus
NPV	nucleus parvicellularis
NSC	nucleus subcoeruleus
PAG	periaqueduct gray

PG	pontine gray
PH	nucleus praepositus hypoglossi
PIA	pontine inhibitory area
PoC, POC	nucleus reticularis pontis caudalis
PPN	pedunculopontine nucleus
PT	pyramidal tract
RN	red nucleus
RRN	retrorubral nucleus
SC	superior colliculus
SN	substantia nigra
SO	superior olivary nucleus
SVN	superior vestibular nucleus
TB	trapezoid body
TRC	tegmental reticular nucleus, central division
TRP	tegmental reticular nucleus, pericentral division
3	oculomotor nucleus
4	trochlear nucleus
4v	fourth ventricle
5MD	motor trigeminal nucleus, dorsal division
5PD	principle sensory trigeminal nucleus, dorsal division
5PV	principle sensory trigeminal nucleus, ventral division
5SM	spinal trigeminal nucleus
5ST	spinal trigeminal tract
7G	genu of the facial nerve
7N	facial nerve

LITERATURE CITED

Beitz AJ, Larson AA, Monaghan P, Altschuler RA, Mullet MM, and Madl JE (1986) Immunohistochemical localization of glutamate, glutaminase, and aspartate aminotransferase in neurons of the pontine nuclei of the rat. Neuroscience 17:741–753. [PubMed: 2422596]

Berman AL (1968) The Brain Stem of the Cat Madison: University of Wisconsin Press.

Fonnum F (1991) Neurochemical studies on glutamate-mediated neuro-transmission. In Meldrum BS, Moroni F, Simon RP, and Woods JH (eds): Excitatory Amino Acids New York: Raven Press, pp. 15–25.

George R, Haslett WL, and Jenden DJ (1964) A cholinergic mechanism in the brainstem reticular formation: Induction of paradoxical sleep. Int. J. Neuropharmacol 3:541–552. [PubMed: 14344492]

Hepler JR, Petrusz P, and Rustioni A (1986) Antisera to GABA, glutamate and aspartate: Characterization by immunoabsorption and immunocytochemistry. J. Histochem. Cytochem 34:110.

Hepler JR, Toomin CS, McCarthy KD, Conti F, Battaglia G, Rustioni A, and Petrusz P (1988) Characterization of antisera to glutamate and aspartate. J. Histochem. Cytochem 36: 13–22. [PubMed: 2891743]

Lai YY, and Siegel JM (1988) Medullary regions mediating atonia. J. Neurosci 8:4790–4796. [PubMed: 2904495]

Lai YY, and Siegel JM (1989) Cardiovascular and muscle tone changes produced by microinjection of cholinergic and glutamatergic agonists in dorsolateral pons and medial medulla. Brain Res 514:27–36.

Lai YY, and Siegel JM (1990) Muscle tone suppression and stepping produced by stimulation of midbrain and rostra1 pontine reticular formation. J. Neurosci 10:2727–2734. [PubMed: 2388085]

Lai YY, and Siegel JM (1991) Pontomedullary glutamate receptors mediating locomotion and muscle tone suppression. J. Neurosci 11:2931–2937. [PubMed: 1679125]

McCarley RW, Ito K, and Rodrigo-Angulo ML (1987) Physiological studies of brainstem reticular connectivity. II. Responses of mPRF neurons to stimulation of mesencephalic and contralateral pontine reticular formation. Brain Res 409:111–127. [PubMed: 3034376]

Mesulam MM (1978) Tetramethyl benzidine for horseradish peroxidase neurohistochemistry: A non-carcinogenic blue reaction product with superior sensitivity for visualizing neural afferents and efferents. J. Histochem. Cytochem 26: 106–117. [PubMed: 24068]

Mesulam M-M, Geula C, Bothwell MA, and Hersh LB (1989) Human reticular formation: Cholinergic neurons of the pedunculopontine and laterodorsal tegmental nuclei and some cytochemical comparisons to forebrain cholinergic neurons. J. Comp. Neurol 281:611–633.

Mitani A, Mitani Y, Hallanger AE, Wainer BH, Kataoka K, and McCarley RW (1988) The laterodorsal and pedunculopontine tegmental nuclei are sources of cholinergic projections to the pontine gigantocellular tegmental field in the cat. Sleep Res 17:10.

Moon Edley S, and Graybiel AM (1983) The afferent and efferent connections of the feline nucleus tegmenti pedunculopontinus, pars compacta. J. Comp. Neurol 217:187–215. [PubMed: 6886052]

Quattrochi JJ, Mamelak AN, Madison RD, Mcklis JD, and Hobson JA (1989) Mapping neuronal inputs to REM sleep induction sites with carbachol-fluorescent microspheres. Science 245:984–986. [PubMed: 2475910]

Reiner PB, and Vincent SR (1987) Topographic relations of cholinergic and noradrenergic neurons in the feline pontomesencephalic tegmentum: An immunohistochemical study. Brain Res. Bull 19:705–714. [PubMed: 2894238]

Rye DB, Saper CB, and Wainer BH (1984) Stabilization of the tetramethylbenzidine (TMB) reaction product: Application for retrograde and anterograde tracing, and combination with immunohistochemistry. J. Histochem. Cytochem 32:1145–1153. [PubMed: 6548485]

Sakai K (1980) Some anatomical and physiological properties of dorsolateral tegmental neurons with special reference in the PGO waves and postural atonia during paradoxical sleep in the cat. In Hobson JA and Brazier MA (eds): The Reticular Formation Revisited New York: Raven Press, pp. 427–447.

Schenck CH, and Mahowald MW (1990) Polysomnographic, neurologic, psychiatric, and clinical outcome report on 70 consecutive cases with REM sleep behavior disorder (RBD): Sustained clonazepam efficacy in 89.5% of 57 treated patients. Cleve. Clin. J. Med 57(Suppl):S9–S23.

Schenck CH, Hopwood J, Duncan E, and Mahowald MW (1992) Preservation and loss of REM-atonia in human idiopathic REM sleep behavior disorder (RBD): Quantitative polysomnographic (PSG) analyses in 17 patients. Assoc. Prof. Sleep Soc. 6th Ann. Meeting, Abstr 27.

Scherer-Singler U, Vincent SR, Kimura H, and McGeer EG (1983) Demonstration of a unique population of neurons with NADPH-diaphorase histochemistry. J. Neurosci. Methods 9:229–234. [PubMed: 6363828]

Semba K, Reiner PB, and Fibiger HC (1990) Single cholinergic mesopontine tegmental neurons project to both the pontine reticular formation and the thalamus in the rat. Neuroscience 38:343–654. [PubMed: 1979854]

Shammah-Lagnado SJ, Negrao N, Silva BA, and Ricardo JA (1987) Afferent connections of the nuclei reticularis pontis oralis and caudalis: A horseradish peroxidase study in the rat. Neuroscience 20:961–989. [PubMed: 2439943]

Shiromani PJ, Siegel JM, Tomaszewski KS, and McGinty DJ (1986) Alterations in blood pressure and REM sleep after pontine carbachol microinfusion. Exp. Neurol 91:285–292. [PubMed: 3943576]

Shiromani PJ, Armstrong DM, and Gillin JC (1988) Cholinergic neurons from the dorsolateral pons project to the medial pons: A WGA-HRP and choline acetyltransferase immunohistochemical study. Neurosci. Lett 95:19–23. [PubMed: 2465510]

Siegel JM, Nienhuis R, Fahringer HM, Paul R, Shiromani P, Dement WC, Mignot E, and Chiu C (1991) Neuronal activity in narcolepsy: Identification of cataplexy related cells in the medial medulla. Science 262:1315–1318.

Siegel JM, Nienhuis R, Fahringer HM, Chiu C, Dement WC, Mignot E, and Lufkin R (1992) Activity of medial mesopontine units during cataplexy and sleep-waking states in the narcoleptic dog. J. Neurosci 12:1640–1646. [PubMed: 1578258]

Tohyama M, Sakai K, Salvert D, Touret M, and Jouvet M (1979) Spinal projections from the lower brainstem in the cat as demonstrated by the horseradish peroxidase technique. I. Origins of the reticulospinal tracts and their funicular trajectories. Brain Res 173:383–403. [PubMed: 487101]

van Dongen PAM, Broekkamp CLE, and Cools AR (1978) Atonia after carbachol microinjections near the locus coeruleus in cat. Pharmacol. Biochem. Behav 8:527–532. [PubMed: 209480]

Vanni-Mercier G, Sakai K, Lin JS, and Jouvet M (1989) Mapping of cholinoceptive brainstem structures responsible for the generation of paradoxical sleep in the cat. Arch. Ital. Biol 127:133–164. [PubMed: 2774793]

Vincent SR, and Kimura H (1992) Histochemical mapping of nitric oxide synthase in the rat brain. Neuroscience 46:755–784. [PubMed: 1371855]

Vincent SR, Satoh K, Armstrong DM, Panula P, Vale W, and Fibiger HC (1986) Neuropeptides and NADPH-diaphorase activity in the ascending cholinergic reticular system of the rat. Neuroscience 17:167–182. [PubMed: 3960309]

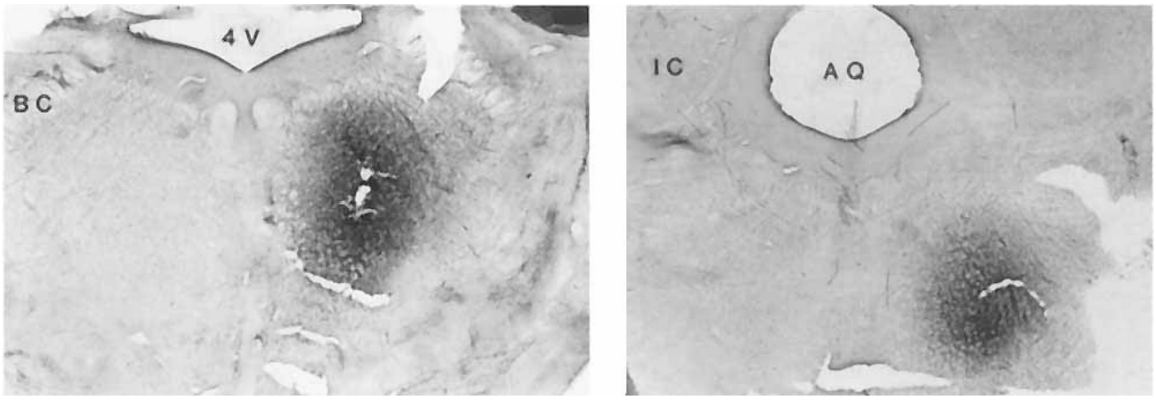

Fig. 1.
Photographs show two examples of injection sites. Magnification: × 2.5.

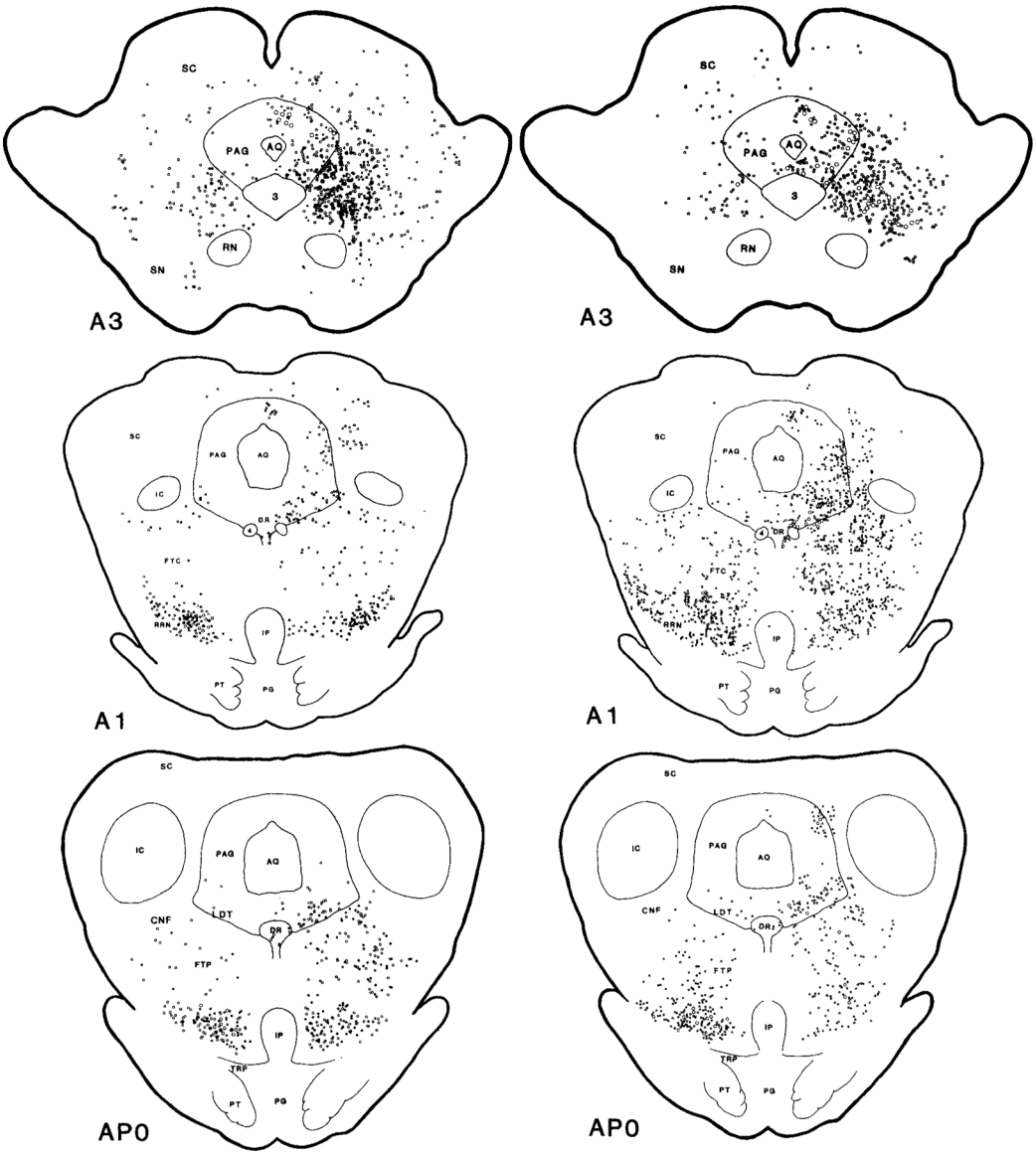

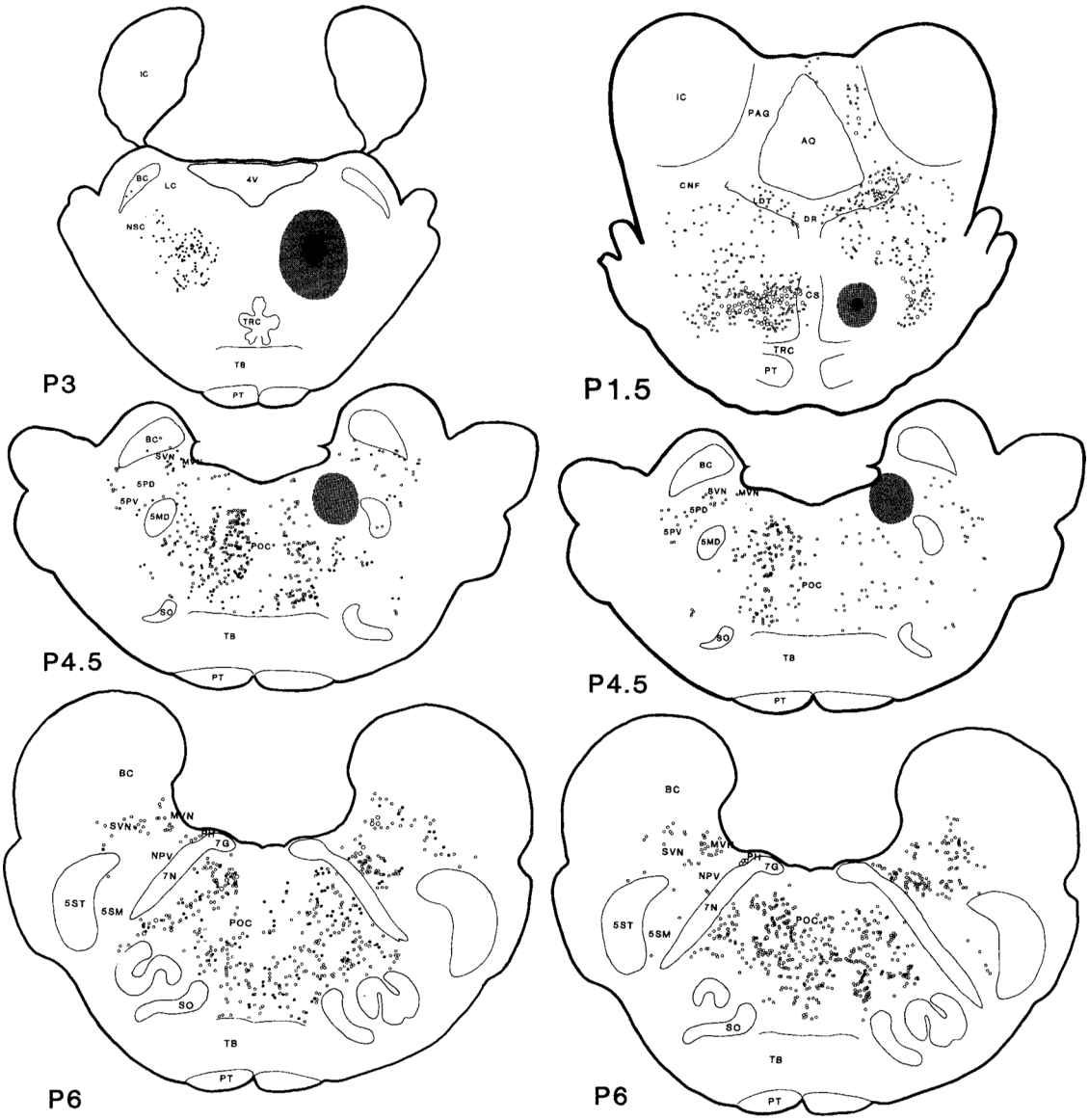

Figs. 2 and 3.

Serial coronal sections of the mesopontine brainstem illustrate the wheat germ agglutinin conjugated horseradish peroxidase (WGA-HRP) labelled projecting neurons also containing NADPH-d (**right**) and glutamate (**left**). Dots represent WGA-HRP neurons double labelled with either NADPH-d or glutamate. Circles represent neurons labelled with WGA-HRP only. The small and large symbols represent one and five neurons, respectively. Each view is based on a 50 μm section from one cat. The black and stippled areas represent the WGA-HRP injection center and diffusion areas, respectively. The histology was reconstructed and the rostrocaudal levels were modified according to Berman's atlas (1968). A, anterior; P, posterior to stereotaxic zero.

Fig. 4.

Photomicrographs showing labelled neurons in the brainstem. Sections shown in a, b, e, f, g, k, and l were processed with tetramethylbenzidine (TMB) and NADPH-d histochemical staining; sections c, d, and j were processed with TMB and glutamate immunohistochemical staining; and sections h and i were stained with TMB, NADPH-d, and glutamate immunohistochemical technique. The areas within the red boxes in a and f are shown at higher magnification in b and e, respectively. **a**: Low power photomicrograph shows the NADPH-d positive (blue) and WGA-HRP (black) neurons in PPN. **b**: Large single labelled NADPH-d positive cholinergic neuron had multiple neuronal processes. Two crystallized WGA-HRP neurons had a relatively smaller size compared with the NADPH-d positive neuron. **c**: Photomicrograph showing two small spindle shaped cells with elongated neuronal processes in RRN. **d**: WGA-HRP negative but glutamate-like immunoreactive giant neurons (white arrowheads) in cPIA. **e**: High power photomicrograph montage shows

the NADPH-d positive (blue) and double labelled NADPH-d positive and WGA-HRP (white arrow) neurons in LDT taken from inset in f. The black crystal of TMB products was mixed in the homogenous blue NADPH-d positive reaction in the double labelled neuron. **g**: Large single labelled WGA-HRP neuron taken from the POC. **h**, **i**: Double labelled glutamate (brown) and NADPH d (blue) immunohistochemical stained neuron taken from the PPN (h, white arrow). **j**: Montage of two single labelled glutamate-like reactive neurons and two double labelled glutamate and WGA-HRP neurons seen in contralateral side of the PIA. **k**: TMB stained crossing fibers from the contralateral side of the PIA projecting to the injection site were seen in the CS area. **l**: Low power photomicrograph showing high density of the projection neurons in ventral part of the FTP. See text for details. Scale bars: a, d, and f = 200 μm; b, e, g, i, and j = 20 μm; c and k = 50 μm; h = 100 μm; 1 = 500 μm.

TABLE 1.

Distribution of Projection Neurons in Brainstem to PIA[1]

Brainstem structures	HRP cells	Glut + HRP cells	NADPH-d[2] + HRP cells	Glut + HRP/HRP × 100%	NADPH-d + HRP/HRP × 100%
cPIA	97	89	0	92	0
FTP	118/202	67/92	0	57/46	0
PPN	114/26	62/7	15/6	54/27	13/23
LDT	89/18	31/3	8/4	35/17	9/22
MRF	412/70	209/17	0	51/24	0
PAG	214/16	69/4	0	32/25	0
RRN	83/157	53/58	0	64/37	0
SC	132/23	36/7	0	25/30	0

[1]The number of projection neurons is based on the average of two animals with caudal injections. Each number was based on four sections from each cat. The numbers on the left and right represent ipsilateral and contralateral projection neurons, respectively. Columns 5 and 6 give the percentage of neurons projecting to PIA that are glutamate and NADPH-d positive, respectively.

[2]NADPH-d positive neurons represent cholinergic neurons in LDT and PPN